Available online at www.sciencedirect.com

ScienceDirect

Journal of the European Ceramic Society 30 (2010) 2003–2008

www.elsevier.com/locate/jeurceramsoc

Crystallization studies in mullite and mullite–YSZ beads

E. Garcia*, J. Mesquita-Guimarães, P. Miranzo, M.I. Osendi

Institute of Ceramics and Glass (ICV), CSIC, Madrid, Spain

Received 29 September 2009; received in revised form 30 March 2010; accepted 10 April 2010
Available online 4 May 2010

Abstract

Mullite and mullite/Y-ZrO_2 (25 and 50 vol.%) beads were produced by thermal spraying in water the corresponding atomised compositions. The amount of amorphous phases in the as-sprayed beads was comparatively determined by X-ray diffraction (XRD) and differential thermal analysis (DTA) methods. Characteristic XRD peaks associated to crystallization of the mullite and Y-ZrO_2 (t) phases were compared with the intensity of the exothermic events in the DTA for each composition. A direct linear relationship between the amount of amorphous phases estimated by XRD methods and the area under DTA peaks per unit mass was found. The crystallization microstructure of the different composition beads after heat treatments was followed by scanning electron microscopy (SEM).

Keywords: Mullite; ZrO_2; X-ray methods; Electron microscopy; Environmental barrier coatings

1. Introduction

Mullite based compositions find interesting applications in high temperature systems. In particular, for next generation of gas turbine engines with parts made of Si_3N_4 or SiC/SiC, which pursue higher working temperatures and efficiency, jointly with a lowering in fuel consumption and emission of green house effect gases. However, these appealing benefits can be hindered by the rapid degradation of those materials in the high temperature environment of gas turbines,[1–3] due to the reaction of the protective silica layer at their surface with the water vapor produced. In a similar way as thermal barrier coatings (TBC) have been used to protect metallic substrates against high temperatures, environmental barrier coatings (EBC) have been proposed to inhibit substrate corrosion in ceramic components. In this sense, mullite has been used as a transitional protective layer for Si-based components owing to its compatibility and close thermal expansion coefficient to these ceramics.[4–6] Mullite coatings processed by thermal spraying techniques normally become moderately amorphous, later crystallizing when heat-treated at $T \geq 1000\,^{\circ}C$, thus producing volume changes and frequently through coating cracks[7–9] that allow further oxidation. Moreover, even fully crystalline mullite coatings exhibited some volatilization of silica in water vapor rich atmospheres at high temperatures.[6–8] Different approaches have been attempted to solve this problem. Specifically, a ZrO_2–7–8 wt.% Y_2O_3 (YSZ) top coat was plasma sprayed over mullite[8,9] but the large mismatch in the coefficient of thermal expansion (CTE) between YSZ and mullite layers caused the fail of the system. Alternatively, special layered systems have been aimed looking for a reduction in thermal stresses through adjustment of CTE between consecutive layers.[9–12] Mathematical modeling of thermally activated time-dependent deformations in functionally graded zirconia-based TBCs has shown that the driving force for interface crack growth may be reduced by the addition of mullite.[13] Alongside, mullite/YSZ mixtures may play an important role as intermediate layers in mullite-based EBC coatings.

For these complex EBC systems, the study of the amorphous phase formation in thermal sprayed mullite/ZrO_2 compositions as well as the effect of ZrO_2 on the crystallization temperature onset are issues of great significance that can help in the successful design and performance understanding of these complex coatings. In the present work, we address these topics using X-ray diffraction (XRD) and differential thermal analysis (DTA) as basic tools. Instead of using thermal sprayed coatings as test specimens, we have chosen beads prepared by flame spraying compositions into water. These beads performed as powders and prevented phenomena like preferred orientation or the inter-

---

* Corresponding author. Tel.: +34 917355840; fax: +34 917355843.
E-mail address: garcia@icv.csis.es (E. Garcia).

0955-2219/$ – see front matter © 2010 Published by Elsevier Ltd.
doi:10.1016/j.jeurceramsoc.2010.04.018

ference of the substrate type on heat treatments. In thermally sprayed coatings, preferred orientation usually appears due to piling up of molten and re-solidified particles (splats) that can produce biased data. Observation of the beads surface after the heat treatments under the scanning electron microscope (SEM) helped to establish the specific crystallization microstructures.

2. Experimental

Mullite powders (Baikalox SASM, Baikowski Chemie, Annecy, France), with a purity of 99% and an average particle size of 1.3 μm, and zirconia stabilized with 7 wt.% Y_2O_3 (Y-TZP) powders (TZ4Y, Tosoh, Tokyo, Japan), 99.95% pure and with an average particle size of 0.3 μm, were the starting materials. Three different suspensions with 30 wt.% of solid content of mullite (M100), 75 vol.% mullite–25 vol.% Y-TZP (M75) and 50 vol.% mullite–50 vol.% Y-TZP (M50) were prepared. Suspensions were done in distilled water adding 0.4 wt.% of a polyelectrolyte dispersant (Dolapix CE 64 CA, Zschimmer-Schwarz, Lahnstein, Germany) and 5 wt.% of a polysaccharide binder (KB 1247, Zschimmer-Schwarz, Lahnstein, Germany), all contents are referred to the solid phase. The thoroughly mixing of all ingredients was assured by using a blade mixer and, subsequently, a continuous attrition mill. Owing to their nature, none of the additives left residues after thermal spraying.

The slurries were spray dried with a rotary atomizer spray dryer (Mobile Minor, Niro Atomizer, Søborg, Denmark) in a co-current flow. Beads were made by flame spraying (FS) corresponding batches of spray dried (SD) powders using an oxygen–acetylene gun (model CastoDyn DS 8000, Eutectic Castolin, Madrid, Spain) into a water filled metal container, at the stand-off distance of 15 cm. Beads were drained and oven dried at 120 °C. To study crystallization, beads were furnace treated at 1000 and 1300 °C for 1 h.

Particle size distributions of the SD powders and as-sprayed beads were determined with a laser diffraction analyzer (Mastersizer S, Malvern, UK). The morphology of the different powders was studied with the SEM (DMS-950 Carl-Zeiss, Oberkochen, Germany). XRD were performed using a Xpert PRO diffractometer (PANalytical, NL) with a $\theta/2\theta$ configuration, in the 10–70° 2θ range, with a step of 0.0165°, a time per step of 50 s and 15 rpm of sample spinning. The DTA was performed with a Simultaneous Thermal Analyzer of Netzch, model 409 (Germany), at a heating rate of 10 °C/min, using alumina standard.

3. Results and discussions

SEM micrographs of the SD agglomerates and the corresponding FS beads are shown in Fig. 1. The SD agglomerates show mostly round porous particles, whereas the beads are compact spheres with a narrower size distribution. The average particle size of SD powders and FS beads was around 26 μm for all compositions as it is reflected in Table 1. In the case of M50 beads, crystallizations are evidenced on the particle surface (Fig. 1(f)).

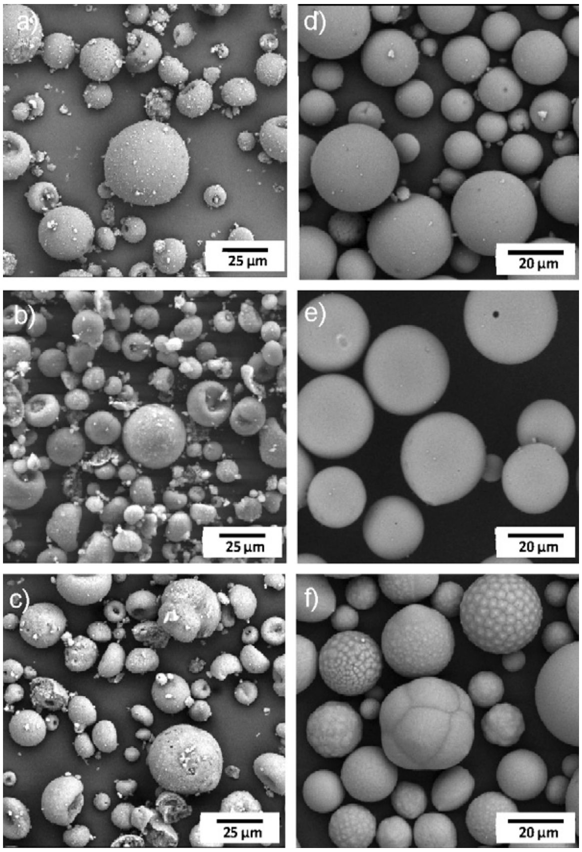

Fig. 1. SD agglomerates and corresponding FS beads of (a and d) M100, (b and e) M75 and (c and f) M50 compositions.

XRD patterns of SD powders and FS beads for the three compositions are compared in Fig. 2 where strong reductions in peaks intensity for the FS beads are evident. M100 SD powders show typical peaks of mullite, whereas M75 SD and M50 SD show intense diffraction peaks of t-ZrO_2 and weak mullite peaks. Furthermore, M100 FS beads show a hump at ∼26° (2θ) indicating the presence of amorphous mullite (Fig. 2(a)); conversely, M50 FS beads present sharp diffraction peak of t-ZrO_2 but mullite diffraction peaks are not detected (Fig. 2(c)). Finally, M75 FS beads are predominantly amorphous (Fig. 2(b)), with a shoulder around 30° (2θ), which corresponds to the maximum intensity peak of t-ZrO_2. The higher amorphisation detected in this composition can be explained by its proximity to the eutectic point of the Al_2O_3–SiO_2–ZrO_2 phase equilibrium diagram[14] as depicted in Fig. 3. Even though thermal spraying methods are very dynamical process, phase equilibrium thermodynamics establishes that eutectic composition is completely melted when eutectic temperature is reached and conversely, on cooling, crystallization occurs at that temperature. Therefore, compositions

Table 1
Average particle size of SD powders and beads.

Composition	SD d_{50} (μm)	FS d_{50} (μm)
M100	26	30
M75	26	28
M50	23	27